# RSS-Based Localization in WSNs Using Gaussian Mixture Model via Semidefinite Relaxation

Yueyue Zhang, *Student Member, IEEE*, Song Xing, *Member, IEEE*, Yaping Zhu, *Student Member, IEEE*, Feng Yan, *Member, IEEE*, and Lianfeng Shen, *Senior Member, IEEE*

***Abstract*— Energy-based source localization methods are normally developed according to the channel path-loss models in which the noise is generally assumed to follow Gaussian distributions. In this letter, we represent the practical additive noise by the Gaussian mixture model, and develop a localization algorithm based on the received signal strength to achieve a maximum likelihood location estimator. By using Jensen's inequality and semidefinite relaxation, the initially proposed nonlinear and nonconvex estimator is relaxed into a convex optimization problem, which can be efficiently solved to obtain the globally optimal solution. Besides, the corresponding Cramer–Rao lower bound is derived for performance comparison. Simulation and experimental results show a substantial performance gain achieved by our proposed localization algorithm in wireless sensor networks.**

***Index Terms*— Received signal strength (RSS), Gaussian mixture model (GMM), semidefinite relaxation.**

## I. Introduction

WIRELESS source localization has attracted considerable attentions over the past decades. Among different localization methods, energy-based localization via received signal strength (RSS) or received signal strength difference (RSSD) enables a simple implementation compared to other conventional technologies such as time of arrival (TOA) [1], time difference of arrival (TDOA) [2], and angle of arrival (AOA) [3]. Recent progress has made it practical to realize the energy-based localization in various networks including wireless sensor networks (WSNs) [4], wireless local area network (WLAN) [5], and vehicular ad-hoc networks (VANETs).

Nevertheless, RSS-based localization to achieve maximum likelihood (ML) estimator of the coordinates of target nodes leads to a nonlinear and nonconvex optimization problem. Several methods have been proposed to address this issue. In [6], for example, a weighed least squares (WLS) formulation has been derived to jointly estimate the sensor node location and the transmit power, based on the unscented transformation (UT). In [4], a proposed estimator approximates the ML estimate for low noise level first, and then is relaxed by applying the efficient convex relaxations that are based on the second-order cone programming (SOCP). And, a semidefinite programming (SDP) estimator has been designed specifically for the RSS-based localization problems [7].

Additionally, it is worth noting that traditional localization algorithm designs in WSNs are based on the classical channel path-loss model with the noise generally modeled by Gaussian distribution. However, in reality the noise does not always follow Gaussian distribution due to the heterogeneity of multiple sources [8]. Hence, the conventional Gaussian model cannot properly represents the measured noise, leading to improper localization algorithms in WSNs. To the best of our knowledge, no study has utilized a practical channel path-loss model with non-Gaussian noise in the node localization algorithms in WSNs.

Motivated by above observations, in this letter we proposed an improved RSS-based node localization algorithm, called Gaussian mixture-semidefinite programming (GM-SDP) estimator, to achieve the ML estimation of the node positions in WSNs. Specifically, the noise is represented by a non-Gaussian model followed by an empirical parameter estimate of the noise. Then we formulate the localization algorithm as an optimization problem to achieve ML performance. The subsequent nonlinear and nonconvex optimization problem is solved by semidefinite relaxation to obtain the suboptimal solution. Finally, both simulation and experimental results illustrate the performance gain of our proposed GM-SDP algorithm over the traditional localization algorithms.

*Notation:* In the paper, $\mathbb{R}^n$ and $\mathbb{S}^n$ denote the set of $n$ vectors and the $n \times n$ symmetric matrix, respectively. In addition, for any symmetric matrix $\mathbf{A}$, $\mathbf{A} \succeq \mathbf{0}$ means that $\mathbf{A}$ is positive semidefinite. $\|\cdot\|_1$, $\|\cdot\|_2$ and $\|\cdot\|_\infty$ denote the $\ell_1$, $\ell_2$ and $\ell_\infty$ vector norms, respectively.

## II. System Model and Preliminaries

Let's denote the unknown coordinates of the $j$th target node as $\boldsymbol{\varphi}_j=[\varphi_{j1}, \varphi_{j2}]^T$ ($\boldsymbol{\varphi}_j \in \mathbb{R}^2, j = 1, \cdots, M$) and the known coordinates of the $i$th anchor node as $\boldsymbol{\alpha}_i=[\alpha_{i1}, \alpha_{i2}]^T$ ($\boldsymbol{\alpha}_i \in \mathbb{R}^2, i = 1, \cdots, N$), where $M$ and $N$ are the total number of targets and anchors, respectively. From [4] and [7], the power received at the $j$th target from the $i$th anchor (or vice versa) is typically modeled as

$$P_{i,j} = P_0 - 10\beta \log_{10} \frac{d(\boldsymbol{\varphi}_j, \boldsymbol{\alpha}_i)}{d_0} + n_{i,j}, \tag{1}$$

where $P_0$ denotes the transmitted power at reference distance $d_0$ from the receiver, $d(\boldsymbol{\varphi}_j, \boldsymbol{\alpha}_i) = \|\boldsymbol{\varphi}_j - \boldsymbol{\alpha}_i\|_2$ is the Euclidean distance between the $j$th target and the $i$th anchor

Manuscript received January 10, 2017; accepted January 30, 2017. Date of publication February 8, 2017; date of current version June 8, 2017. This work was supported by the National Natural Science Foundation of China (No. 61471164, 61601122), the Innovation Project of Jiangsu Province (KYLX16 0222), and the Research Fund of National Mobile Communications Research Laboratory (NCRL), Southeast University (SEU) (No. 2016B02). The associate editor coordinating the review of this letter and approving it for publication was L. Mucchi. *(Corresponding author: Lianfeng Shen.)*

Y. Zhang, Y. Zhu, F. Yan, and L. Shen are with the National Mobile Communications Research Laboratory, Southeast University, Nanjing 210096, China (e-mail: douleyue@seu.edu.cn; xyzzyp@seu.edu.cn; feng.yan@seu.edu.cn; lfshen@seu.edu.cn).

S. Xing is with the Department of Information Systems, California State University, Los Angeles, CA 90032 USA (e-mail: sxing@exchange.calstatela.edu).

Digital Object Identifier 10.1109/LCOMM.2017.2666157

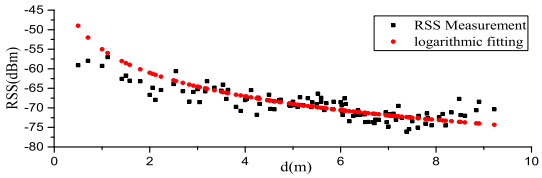


(a) A comparison between the empirical path loss model without noise and the real RSS measurements.

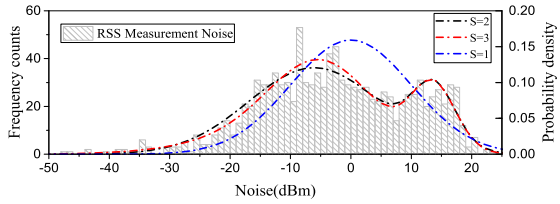


(b) Histogram of the experimental RSS measurement noise and different distributive profiles.

Fig. 1. Experimental measurements analysis.

node, $\beta$ is a path-loss exponent with the common value between 2 and 6, and the additive noise $n_{i,j}$ following the Gaussian distribution represents the log-normal shadowing effect in multipath environments, respectively.

However, there are two related issues with (1). One is related to RSS level behavior which is illustrated in Fig. 1 (a). We adopt the logarithmic curve for the fitting of the RSS measurements. Another is as mentioned in Section I that $n_{i,j}$ may not always follow Gaussian distributions in real environment. In this letter, we aim at developing an improved channel path-loss model by capturing the characteristics of the additive noise, which is shown by the histogram of the RSS measurement noise in Fig. 1 (b).

Here, we represent the noise with a Gaussian mixture model (GMM) and the resulting joint conditional probability distribution function (pdf) of observed power vector $\boldsymbol{P}_j = [P_{1,j}, \ldots, P_{N,j}]$ at the $j$th target is

$$p(\boldsymbol{P}_j|\boldsymbol{\varphi}_j) = \prod_{i=1}^{N}\sum_{s=1}^{S}\tau_{i,s}\mathcal{N}(\mu_s, \sigma_s^2), \tag{2}$$

where $\tau_{i,s}$ is the corresponding weight of the cluster $s$ with mean $\mu_s$ and variance $\sigma_s^2$ of the noise, and $S$ is the number of mixture component.

*Remark:* The path-loss exponent $\beta$ is known and fixed a priori via the simulations and experiments. By using prior experimental measurements, $P_0$ and $\beta$ can be estimated by the logarithmic fitting, and fixed as $P_0 = -55$ dBm and $\beta = 2$, respectively.

## III. Problem Formulation and Solution

In practice, the variables $\mu_s, \sigma_s^2$ and $\tau_{i,s}$ in (2) need to be estimated in the localization process. In the ECM criterion [1], both $\mu_s^{(\eta)}$ and $\sigma_s^{2,(\eta)}$ at the $\eta$th iteration are estimated for updating the position $\boldsymbol{\varphi}_j^{(\eta)}$ but not $\tau_{i,s}^{(\eta)}$. In this letter, both $\boldsymbol{\varphi}_j^{(\eta)}$ and $\tau_{i,s}^{(\eta)}$ would be jointly optimized. For the sake of convenience, the index of the iteration $\eta$ is not shown.

To this end, the objective of designing the localization algorithm via GM-SDP is to obtain the ML estimate $\boldsymbol{\varphi}_j^*$ by finding the parameter $\tau_{i,s}$. Then the ML estimator can be formulated as

$$\begin{aligned}&\max_{\boldsymbol{\varphi}_j,\boldsymbol{\tau}}\ \Phi(\boldsymbol{\varphi}_j,\boldsymbol{\tau})\\ &\text{s.t. C1}: \Sigma_{s=1}^{S}\tau_{i,s} = 1, \quad \forall i\\ &\quad \text{C2}: 0 \le \tau_{i,s} \le 1, \quad \forall s, i\\ &\quad \text{C3}: d(\boldsymbol{\varphi}_j, \boldsymbol{\alpha}_i) \ne 0, \quad \forall i,\end{aligned} \tag{3}$$

where $\Phi(\boldsymbol{\varphi}_j,\boldsymbol{\tau})$ is the log-likelihood function of the joint conditional pdf in (2), i.e., $\Phi(\boldsymbol{\varphi}_j,\boldsymbol{\tau}) = \ln p(\boldsymbol{P}_j|\boldsymbol{\varphi}_j)$, and the mixture weights $\tau_{i,s}$ is constrained to sum up to 1.

However, the combinatorial nature of the objective function in (3) results in an NP-hard problem. To reduce the complexity, the optimization problem can be reformulated by finding a lower bound of the original non-convex objective function. Then, the reformulated problem is solved as an SDP problem via the relaxation to obtain the globally optimal solution. To be concrete, we start to solve the original problem in (3) by obtaining a suboptimal solution via the following proposition.

*Proposition 1:* For a feasible pair $(\boldsymbol{\varphi}_j,\boldsymbol{\tau})$, if the pair is an optimal solution to the following optimization problem

$$\begin{aligned}&\max_{\boldsymbol{\varphi}_j}\ \sum_{i=1}^{N}\sum_{s=1}^{S}\tau_{i,s}\ln\mathcal{N}(\mu_s,\sigma_s^2)\\ &\text{s.t. C1, C2, C3,}\end{aligned} \tag{4}$$

the feasible pair $(\boldsymbol{\varphi}_j,\boldsymbol{\tau})$ is *suboptimal* for the primal problem in (3).

*Proof:* The optimal value of $\boldsymbol{\varphi}_j$ in (3) is defined as $\Phi^* = \sup\{\Phi(\boldsymbol{\varphi}_j,\boldsymbol{\tau})|\text{C1, C2, C3}\}$, and a feasible solution $(\boldsymbol{\varphi}_j,\boldsymbol{\tau})$ is $\epsilon - suboptimal$ if $\Phi(\boldsymbol{\varphi}_j,\boldsymbol{\tau}) \ge \Phi^* - \epsilon$. Using Jensen's inequality, the lower bound of the primal non-convex weighted objective function of (3) can be obtained and given by

$$\Phi(\boldsymbol{\varphi}_j,\boldsymbol{\tau}) \ge \sum_{i=1}^{N}\sum_{s=1}^{S}\tau_{i,s}\ln\mathcal{N}(\mu_s,\sigma_s^2) = \Phi_1(\boldsymbol{\varphi}_j,\boldsymbol{\tau}). \tag{5}$$

Obviously, $\Phi_1(\boldsymbol{\varphi}_j,\boldsymbol{\tau})$ serves as a lower bound for the log-likelihood function of the parameters $(\boldsymbol{\varphi}_j,\boldsymbol{\tau})$. Hence, there always exists $\epsilon'$ that makes $(\boldsymbol{\varphi}_j,\boldsymbol{\tau})$ satisfy $\Phi_1(\boldsymbol{\varphi}_j,\boldsymbol{\tau}) \ge \Phi^* - \epsilon'$. Therefore, $(\boldsymbol{\varphi}_j,\boldsymbol{\tau})$ is $\epsilon' - suboptimal$ for the problem in (3) and the proposition holds. Furthermore, the optimization problem in (3) can be reformed as

$$\begin{aligned}&\min_{\boldsymbol{\varphi}_j,\boldsymbol{\tau}}\ \Phi_2(\boldsymbol{\varphi}_j,\boldsymbol{\tau})\\ &\text{s.t. C1, C2, C3,}\end{aligned} \tag{6}$$

where

$$\begin{aligned}\Phi_2(\boldsymbol{\varphi}_j,\boldsymbol{\tau}) &= -\Phi_1(\boldsymbol{\varphi}_j,\boldsymbol{\tau})\\ &= \sum_{i=1}^{N}\sum_{s=1}^{S}\tau_{i,s}\left[\ln\sqrt{2\pi}\sigma_s + \frac{(n_{i,j}-\mu_s)^2}{2\sigma_s^2}\right].\end{aligned} \tag{7}$$

Clearly, the objective in (6) is non-convex since its domain $\{\boldsymbol{\varphi}_j|\boldsymbol{\varphi}_j \ne \boldsymbol{\alpha}_i\}$ is not continuous, and $\log_{10}\frac{d(\boldsymbol{\varphi}_j,\boldsymbol{\alpha}_i)}{d_0}$ is not convex on the convex domain. Hence, it is difficult to find the globally optimal solution to the problem in (6). To achieve a convex estimator in (6), we introduce the following lemma.

Lemma *1:* If $\boldsymbol{x} \in \mathbb{R}^n$, we have

1) $\|\boldsymbol{x}\|_\infty \le \|\boldsymbol{x}\|_2 \le \sqrt{n}\|\boldsymbol{x}\|_\infty$, 2) $\|\boldsymbol{x}\|_\infty \le \|\boldsymbol{x}\|_1 \le n\|\boldsymbol{x}\|_\infty$.

By replacing the $\ell_2$ norm in $\Phi_2$ with the $\ell_\infty$ norm, i.e., the Chebyshev norm, we have

$$\begin{aligned}\frac{(n_{i,j}-\mu_s)^2}{2\sigma_s^2} &\overset{(a)}{\Leftrightarrow} \max\left|\frac{1}{\sigma_s}\log_{10}\frac{d^2(\boldsymbol{\varphi}_j,\boldsymbol{\alpha}_i)}{\gamma_{i,s}^2}\right| \\ &\overset{(b)}{\Longleftrightarrow} \max\left[\frac{d^2(\boldsymbol{\varphi}_j,\boldsymbol{\alpha}_i)}{\sigma_s\gamma_{i,s}^2}, \frac{\gamma_{i,s}^2}{\sigma_s d^2(\boldsymbol{\varphi}_j,\boldsymbol{\alpha}_i)}\right] \triangleq \xi_{i,s},\end{aligned} \tag{8}$$

where $\gamma_{i,s}^2 = d_0^2 10^{\frac{P_0+\mu_s-P_{i,j}}{5\beta}}$. In (8), (a) results due to 1) in *Lemma*, and (b) results based on that $\log_{10} x$ is a strictly monotonic function when it is increasing in its entire domain $(0,+\infty)$. Then the primal optimization problem in (6) can be expressed as

$$\begin{aligned}&\min_{\boldsymbol{\varphi}_j,\boldsymbol{\tau},\boldsymbol{\xi}} \sum_{i=1}^{N}\left[\mathrm{Tr}(\boldsymbol{\tau}_i\boldsymbol{\eta}^T)+\mathrm{Tr}(\boldsymbol{\tau}_i\boldsymbol{\xi}_i^T)\right] \\ &\text{s.t. C1, C2, C3} \\ &\quad \mathrm{C4}: \|\boldsymbol{\varphi}_\mathrm{j}-\boldsymbol{\alpha}_\mathrm{i}\|_2^2 \le \gamma_{\mathrm{i,s}}^2\sigma_\mathrm{s}\xi_{\mathrm{i,s}} \\ &\quad \mathrm{C5}: \|\boldsymbol{\varphi}_\mathrm{j}-\boldsymbol{\alpha}_\mathrm{i}\|_2^2 \ge \gamma_{\mathrm{i,s}}^2\sigma_\mathrm{s}^{-1}\xi_{\mathrm{i,s}}^{-1}, \forall \mathrm{i, s}\ ,\end{aligned} \tag{9}$$

where

$$\begin{aligned}\boldsymbol{\tau}_i &= [\tau_{i,1},\ldots,\tau_{i,S}]^T, \\ \boldsymbol{\eta} &= [\ln\sqrt{2\pi}\sigma_1,\ldots,\ln\sqrt{2\pi}\sigma_S]^T, \\ \boldsymbol{\xi}_i &= [\xi_{i,1},\ldots,\xi_{i,S}]^T.\end{aligned}$$

Noting that $\|\boldsymbol{\varphi}_j-\boldsymbol{\alpha}_i\|_2^2 = \mathrm{Tr}(\boldsymbol{\Psi}) - 2\boldsymbol{\varphi}_j^T\boldsymbol{\alpha}_i + \|\boldsymbol{\alpha}_i\|_2^2$. Hence we rewrite the reformulated problem in norm form as

$$\begin{aligned}&\min_{\boldsymbol{\varphi}_j,\boldsymbol{\tau},\boldsymbol{\xi}} \|\boldsymbol{x}\|_1+\|\boldsymbol{y}\|_1 \\ &\text{s.t. C1, C2, C3} \\ &\quad \mathrm{C4}: \mathrm{Tr}(\boldsymbol{\Psi}) - 2\boldsymbol{\varphi}_\mathrm{j}^\mathrm{T}\boldsymbol{\alpha}_\mathrm{i} + \|\boldsymbol{\alpha}_\mathrm{i}\|_2^2 \le \gamma_{\mathrm{i,s}}^2\sigma_\mathrm{s}\xi_{\mathrm{i,s}} \\ &\quad \mathrm{C5}: \mathrm{Tr}(\boldsymbol{\Psi}) - 2\boldsymbol{\varphi}_\mathrm{j}^\mathrm{T}\boldsymbol{\alpha}_\mathrm{i} + \|\boldsymbol{\alpha}_\mathrm{i}\|_2^2 \ge \gamma_{\mathrm{i,s}}^2\sigma_\mathrm{s}^{-1}\xi_{\mathrm{i,s}}^{-1}, \quad \forall \mathrm{i, s} \\ &\quad \mathrm{C6}: \boldsymbol{\Psi} = \boldsymbol{\varphi}_\mathrm{j}\boldsymbol{\varphi}_\mathrm{j}^\mathrm{T}, \boldsymbol{\Psi}\in\mathbb{S}^2 \\ &\quad \mathrm{C7}: \mathrm{x_i} = \mathrm{Tr}(\boldsymbol{\tau}_\mathrm{i}\boldsymbol{\eta}^\mathrm{T}) \\ &\quad \mathrm{C8}: \mathrm{y_i} = \mathrm{Tr}(\boldsymbol{\tau}_\mathrm{i}\boldsymbol{\xi}_\mathrm{i}^\mathrm{T}), \quad \forall \mathrm{i}.\end{aligned} \tag{10}$$

However, the problem in (10) is still non-convex since the equality constraints C6 and C8 are not affine. To obtain a convex optimization problem in (10), we relax C6 into an inequality constraint $\boldsymbol{\Psi} \succeq \boldsymbol{\varphi}_j\boldsymbol{\varphi}_j^T$ (semidefinite relaxation), and relax C8 into $y_i = \sum_{s=1}^{S}\tau_{i,s}\xi_{i,s} \ge \sum_{s=1}^{S}\xi_{i,s}$ (Jensen's inequality). Further, using Schur complement, the constraints C5 and C6 in (10) can be expressed in a linear matrix inequality (LMI) [9], shown in the rewritten optimization problem as below.

$$\begin{aligned}&\min_{\boldsymbol{\varphi}_j,\boldsymbol{\tau},\boldsymbol{\xi}} \|\boldsymbol{x}\|_1+\|\boldsymbol{y}\|_1 \\ &\text{s.t. C1, C2, C3, C4} \\ &\quad \mathrm{C5}: \begin{bmatrix}\mathrm{Tr}(\boldsymbol{\Psi}) - 2\boldsymbol{\varphi}_j^T\boldsymbol{\alpha}_i + \|\boldsymbol{\alpha}_i\|_2^2 & \gamma_{i,s}/\sqrt{\sigma_s} \\ \gamma_{i,s}/\sqrt{\sigma_s} & \xi_{i,s}\end{bmatrix} \ge 0, \quad \forall \mathrm{i, s} \\ &\quad \mathrm{C6}: \begin{bmatrix}\boldsymbol{\Psi} & \boldsymbol{\varphi}_j \\ \boldsymbol{\varphi}_j^T & 1\end{bmatrix} \ge 0, \boldsymbol{\Psi}\in\mathbb{S}^2 \\ &\quad \mathrm{C7}: \mathrm{x_i} \ge \mathrm{Tr}(\boldsymbol{\tau}_\mathrm{i}\boldsymbol{\eta}^\mathrm{T}) \quad \mathrm{C8}: \mathrm{y_i} \ge \sum_{\mathrm{s=1}}^{\mathrm{S}}\xi_{\mathrm{i,s}}, \quad \forall \mathrm{i, s}.\end{aligned} \tag{11}$$

Now (11) is a convex optimization problem, which can be solved by the existing numerical tools [10] to obtain the globally optimal solution $\boldsymbol{\varphi}_j^*$ of the original optimization problem in (3).

## IV. Cramer-Rao Lower Bound on Estimator Variance

It is easily found that our GM-SDP estimator $\widehat{\boldsymbol{\varphi}}(\boldsymbol{P})$ is unbiased, i.e., $\mathbb{E}[\widehat{\boldsymbol{\varphi}}(\boldsymbol{P})] = \boldsymbol{\varphi}(\boldsymbol{P})$. The accuracy of an estimator may be illustrated by some costs associated with the estimate. The most commonly used cost is the mean squared error (MSE), or the estimator variance for an unbiased estimate. It is well known that the Cramer-Rao lower bound (CRLB), which is the inverse of the Fisher information matrix (FIM), represents a lower bound on the variance of any unbiased estimators. Specifically, the variance of our GM-SDP estimator will meet

$$\mathbb{E}\left\{[\widehat{\boldsymbol{\varphi}}(\boldsymbol{P})-\boldsymbol{\varphi}]\,[\widehat{\boldsymbol{\varphi}}(\boldsymbol{P})-\boldsymbol{\varphi}]^T\right\} \succeq \mathcal{J}^{-1}, \tag{12}$$

where the element $[\mathcal{J}]_{v,r}$ of FIM $\mathcal{J}$ is defined by

$$[\mathcal{J}]_{v,r} = \mathbb{E}\left[\frac{\partial \ln p(\boldsymbol{P}_j|\boldsymbol{\varphi}_j)}{\partial\varphi_{j,v}}\cdot\frac{\partial \ln p(\boldsymbol{P}_j|\boldsymbol{\varphi}_j)}{\partial\varphi_{j,r}}\right], v, r\in\mathcal{V}. \tag{13}$$

In(13), $\mathcal{V}$ is denoted as the set of dimensions in the coordinate axis. For a specific target node in our two-dimensional scenario ($|\mathcal{V}|=2$), we have

$$[\mathcal{J}]_{v,r} = \left[\frac{10\beta}{\ln 10}\right]^2 I_n\sum_{i=1}^{N}\frac{(\varphi_{j,v}-\alpha_{i,v})(\varphi_{j,r}-\alpha_{i,r})}{\|\boldsymbol{\phi}_j-\boldsymbol{\alpha}_i\|_2^4}, v, r\in\mathcal{V}, \tag{14}$$

where

$$I_n = \mathbb{E}\left\{\left[\frac{\nabla_n p(n)}{p(n)}\right]^2\right\} = \int\frac{[\nabla_n p(n)]^2}{p(n)}\,\mathrm{d}n. \tag{15}$$

In (15), $p(n)\sim\sum_{s=1}^{S}\tau_s\mathcal{N}(\mu_s,\sigma_s^2)$, and $I_n$ can be evaluated numerically by Monte Carlo integration [1]. Further, by defining the location estimation error as $e = \|\widehat{\boldsymbol{\varphi}}-\boldsymbol{\varphi}\|_2$, its root mean square error (RMSE) is lower bounded by [7]

$$\sqrt{\mathbb{E}(e^2)} \ge \sqrt{\mathrm{Tr}[\mathcal{J}^{-1}]} \triangleq \mathbf{CRLB}(\boldsymbol{\varphi}). \tag{16}$$

## V. Results Analysis

### A. Simulation Results: Influence of the Number of Anchors

Numerical simulations are conducted to evaluate the performance of our proposed GM-SDP algorithm. We consider a two-dimensional square region with the size of $15\times 15$ m$^2$ for the simulations. In the network, 120 sensors (including 20 anchors) are uniformly deployed. Due to space limit, the detailed strategy for anchor selection is omitted. The noise is assumed to follow a two-mode Gaussian mixture distribution with $\tau_1 = 0.37$, $\mu_1 = -4.36$ dBm, $\sigma_1 = 5.22$ dBm, $\tau_2 = 0.63$, $\mu_2 = 1.73$ dBm, $\sigma_2 = 4.09$ dBm. Here, the setting of the mean and variance of each mixture component is an example of the realistic indoor noise measurements as mentioned in Section I. The performance is evaluated in terms of RMSE

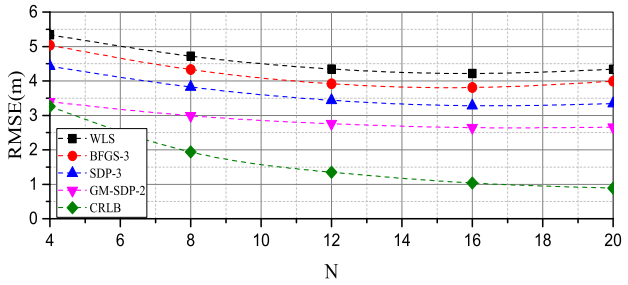


(a) RMSE versus the number of anchors.

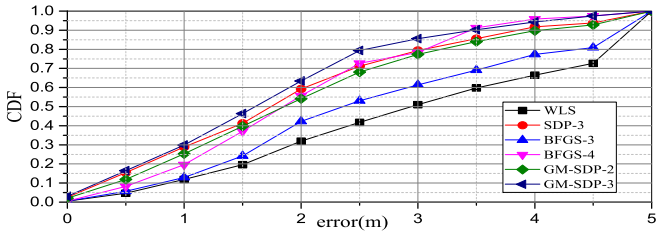


(b) CDF of localization errors for the different algorithms.

Fig. 2. Localisation performance of the different algorithms.

using 100 Monte Carlo runs with the number of anchors varying from 4 to 20.

Fig. 2 (a) illustrates the RMSE vs. the number of anchors for various estimators including BFGS [1], WLS [6], SDP [7], and our proposed GM-SDP. CRLB value is also illustrated in Fig. 2 (a) for comparison. It shows that increasing the number of anchors generally improves the estimate accuracy of all algorithms, revealing that more position information gained from the anchors will help for the accurate RSS measurements. Clearly, our proposed GM-SDP with only fewer mixture components needed to be measured for GMM performs much better than other compared algorithms, which is indicated from the closest RMSE of GM-SDP to CRLB.

### *B. Experimental Results*

The performance of proposed GM-SDP algorithm is further evaluated by the experiments in a real wireless sensor network with RSS measurements. Without loss of generality, five Zigbee nodes (TI-CC2530), among which one is the target node and the other four are anchors, are used in the experiments. The network environment is a typical meeting room where the anchors are fixed at the corners of the room with the coordinates (0, 0) m, (6, 0) m, (6, 7) m, and (0, 7) m, respectively. The RSS measurements are randomly collected in 195 different locations of this area. Fig. 2 (b) illustrates the CDF of the localization estimation errors of various algorithms including GM-SDP. It shows that the performance of SDP-3 estimator is close to GM-SDP-2 and BFGS-4, and BFGS-4 performs better than BFGS-3 due to its approximation of the probability density of the measurement noise with more Gaussian components. For the same reason as BFGS-4 vs. BFGS-3, our proposed GM-SDP-3 provides the better performance than GM-SDP-2. More importantly, GM-SDP-3 performs the best among all algorithms and even more than 63.08% of its localization estimation errors are within a very short range of 2 m.

TABLE I
LOCALIZATION ACCURACY OF DIFFERENT ALGORITHMS

| Methods | RMSE(m) | Maximum Error(m) | $p(\|e\| \leq 2m)$ |
|---|---|---|---|
| WLS | 3.43 | 15.58 | 31.79% |
| SDP-3 | 2.23 | 8.71 | 59.28% |
| BFGS-3 | 2.96 | 13.90 | 42.05% |
| BFGS-4 | 1.83 | 7.63 | 55.38% |
| GM-SDP-2 | 2.06 | 9.86 | 53.84% |
| GM-SDP-3 | 1.67 | 6.56 | 63.08% |

The numerical results in Table I illustrate clearly the performance comparison of various estimators on the experiments. From Table I, we observe that GM-SDP-3 performs the best with the least value of RMSEs and the maximum localization estimation errors among all methods. In addition, the GM-SDP estimator with 2-component performs even better than BFGS with 3-component GMM, which has shown the robustness of the ECM estimate of the noise parameters and also confirmed the observations in [1].

## VI. CONCLUSION

In this letter, the additive noise in RSS measurement is modeled by the Gaussian mixture model, and an improved node localization algorithm employing relaxations is proposed to achieve ML estimate of the node locations in wireless source localization systems, in which the primal nonlinear and nonconvex optimization problem is transformed into a SDP problem to obtain the globally optimal solution. Simulation and experimental results are presented to confirm the performance improvement of the proposed GM-SDP algorithm.

## REFERENCES

[1] F. Yin, C. Fritsche, D. Jin, F. Gustafsson, and A. M. Zoubir, "Cooperative localization in WSNs using Gaussian mixture modeling: Distributed ECM algorithms," *IEEE Trans. Signal Process.*, vol. 63, no. 6, pp. 1448–1463, Mar. 2015.

[2] Y. Liu, F. Guo, L. Yang, and W. Jiang, "An improved algebraic solution for TDOA localization with sensor position errors," *IEEE Commun. Lett.*, vol. 19, no. 12, pp. 2218–2221, Dec. 2015.

[3] S.-F. Chuang, W.-R. Wu, and Y.-T. Liu, "High-resolution AoA estimation for hybrid antenna arrays," *IEEE Trans. Antennas Propag.*, vol. 63, no. 7, pp. 2955–2968, Jul. 2015.

[4] S. Tomic, M. Beko, and R. Dinis, "RSS-based localization in wireless sensor networks using convex relaxation: Noncooperative and cooperative schemes," *IEEE Trans. Veh. Technol.*, vol. 64, no. 5, pp. 2037–2050, May 2015.

[5] W.-Y. Hu, J.-L. Lu, S. Jiang, W. Shu, and M.-Y. Wu, "WiBEST: A hybrid personal indoor positioning system," in *Proc. IEEE WCNC*, Apr. 2013, pp. 2149–2154.

[6] G. Wang, H. Chen, Y. Li, and M. Jin, "On received-signal-strength based localization with unknown transmit power and path loss exponent," *IEEE Wireless Commun. Lett.*, vol. 1, no. 5, pp. 536–539, Oct. 2012.

[7] R. W. Ouyang, A. K.-S. Wong, and C.-T. Lea, "Received signal strength-based wireless localization via semidefinite programming: Noncooperative and cooperative schemes," *IEEE Trans. Veh. Technol.*, vol. 59, no. 3, pp. 1307–1318, Mar. 2010.

[8] D. Wu, Y. Zhang, L. Bao, and A. C. Regan, "Location-based crowdsourcing for vehicular communication in hybrid networks," *IEEE Trans. Intell. Transp. Syst.*, vol. 14, no. 2, pp. 837–846, Jun. 2013.

[9] S. P. Boyd and L. Vandenberghe, *Convex Optimization*. Cambridge, U.K.: Cambridge Univ. Press, 2004.

[10] M. C. Grant and S. P. Boyd. (Oct. 2016). *The CVX Users' Guide Release 2.1*. [Online]. Available: http://cvxr.com/cvx/doc/CVX.pdf